ACS SENSORS

pubs.acs.org/acssensors Article

Rapid Gel Card Agglutination Assays for Serological Analysis Following SARS-CoV-2 Infection in Humans

Diana Alves, Rodrigo Curvello, Edward Henderson, Vidhishri Kesarwani, Julia A. Walker, Samuel C. Leguizamon, Heather McLiesh, Vikram Singh Raghuwanshi, Hajar Samadian, Erica M. Wood, Zoe K. McQuilten, Maryza Graham, Megan Wieringa, Tony M. Korman, Timothy F. Scott, Mark M. Banaszak Holl, Gil Garnier,* and Simon R. Corrie*

Cite This: https://dx.doi.org/10.1021/acssensors.0c01050 Read Online

ACCESS | Metrics & More | Article Recommendations | Supporting Information

ABSTRACT: High-throughput and rapid serology assays to detect the antibody response specific to severe acute respiratory syndrome-coronavirus-2 (SARS-CoV-2) in human blood samples are urgently required to improve our understanding of the effects of COVID-19 across the world. Short-term applications include rapid case identification and contact tracing to limit viral spread, while population screening to determine the extent of viral infection across communities is a longer-term need. Assays developed to address these needs should match the ASSURED criteria. We have identified agglutination tests based on the commonly employed blood typing methods as a viable option. These blood typing tests are employed in hospitals worldwide, are high-throughput, fast (10−30 min), and automated in most cases. Herein, we describe the application of agglutination assays to SARS-CoV-2 serology testing by combining column agglutination testing with peptide−antibody bioconjugates, which facilitate red cell cross-linking only in the presence of plasma containing antibodies against SARS-CoV-2. This simple, rapid, and easily scalable approach has immediate application in SARS-CoV-2 serological testing and is a useful platform for assay development beyond the COVID-19 pandemic.

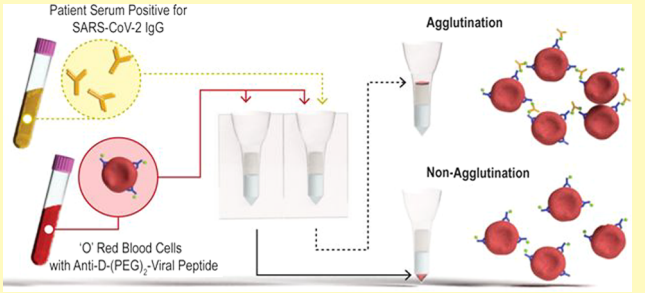

KEYWORDS: *SARS-CoV-2, COVID-19, serology, antibody, column agglutination test, bioconjugate, peptide, clinical samples*

Coronavirus disease (COVID-19) due to severe acute respiratory syndrome-coronavirus-2 (SARS-CoV-2) has caused a worldwide viral pandemic, with >558 085 deaths and >12 419 643 cases reported internationally,[1] with Australia reporting 9359 cases and 106 deaths,[2] as of 10th July 2020. Large-scale efforts are underway to develop vaccines and antiviral therapy, epidemiological methods of social distancing and quarantine are being used to reduce the spread of infection, and the rapid development and deployment of diagnostic tests is of key importance.[3,4] Polymerase chain reaction (PCR) tests are already widely available to confirm SARS-CoV-2 infection from respiratory samples,[3] and direct antigen assays are also emerging to detect current infection.[5,6] However, there is currently a lack of high-throughput, lab-based blood screening tests that detect the antibody response to viral infection. These serology tests are required for population screening, case identification, contact tracing, and potentially to confirm vaccine efficacy during clinical trials and vaccine distribution.[7−9] While the full picture of the immune response to SARS-CoV-2 is still emerging, recent reports suggest that IgG and IgM antibodies are produced either sequentially or simultaneously, with titers reaching a plateau 6 days after seroconversion,[10] and that SARS-CoV-2 antigens elicit highly specific antibody responses not present in naïve individuals, including those previously infected with other coronaviruses.[11,12] A key unanswered question is whether or not SARS-CoV-2 infection yields long-lived antibody responses for long-term protective immunity; mass serology testing is required to comprehensively address this question.

Several approaches for serology testing are already being distributed around the world. Point-of-care paper-based tests for antibodies are under evaluation and available in some countries, but they cannot be used for high-throughput screening (15−30 min/sample), and specificity/sensitivity is not expected to meet the standard of laboratory-based tests. The current gold standard for serology methods is laboratory-based indirect enzyme-linked immunosorbent assay (ELISA), in which antibodies from patient serum are captured onto a

Received: May 24, 2020
Accepted: July 2, 2020

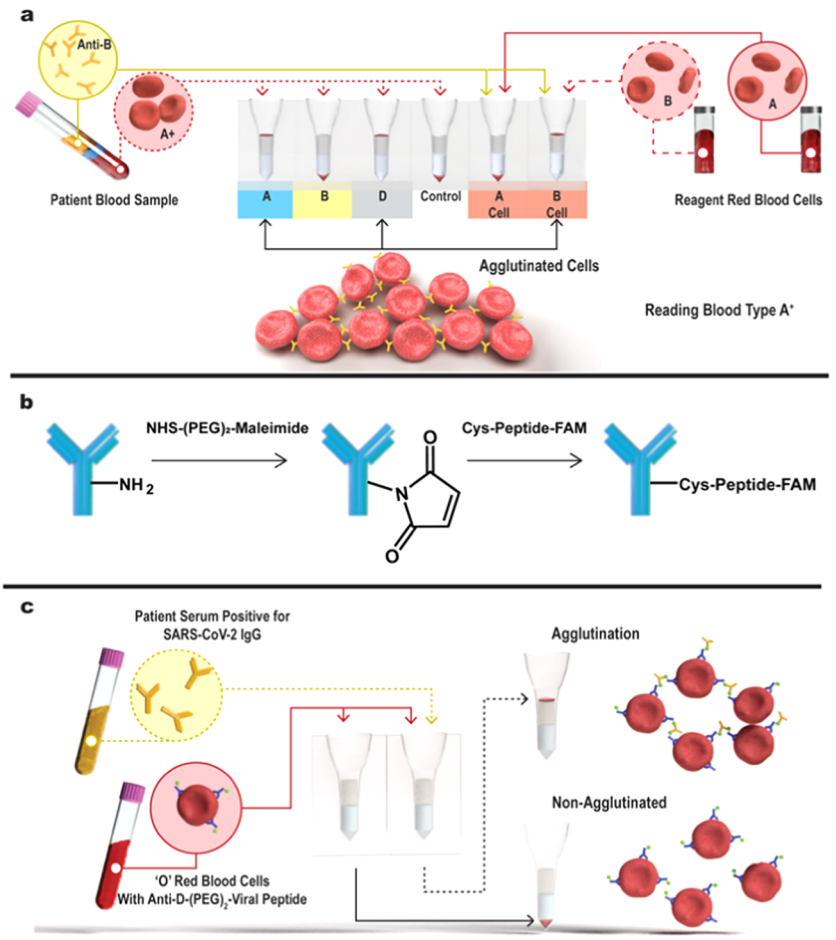

Figure 1. Schematic of blood typing CAT assay and the introduction of antibody−peptide bioconjugates to produce SARS-CoV-2 serology assay. (a) In a typical blood typing assay, RRBCs are incubated with patient samples on a gel card prior to centrifugation to generate a pattern of agglutination results to determine a blood type. (b) Reaction scheme employed to produce the antibody−peptide bioconjugate in a two-step process. (c) In the SARS-CoV-2 serology assay, antibody−peptide bioconjugate-coated RRBCs are incubated with a patient plasma or serum sample on neutral gel card prior to centrifugation to separate agglutinated RRBCs from free RRBCs for visual inspection.

protein-coated microwell plate followed by enzymatic detection using an anti-Ig secondary antibody.[3,4] These assays can be performed manually or using automated systems;[13] however, they are still multistep processes requiring multiple antibodies and reagents.

Alternative approaches should meet the ASSURED (affordable, sensitive, specific, user-friendly, rapid/robust, equipment-free, deliverable to end-users) criteria[14] and be rapidly scalable and customizable. Blood typing and antibody screening are performed in hospital laboratories all over the world, using the robust column agglutination test (CAT) technology. Detection of antibodies in patient plasma or serum involves pipetting a mixture of reagent red blood cells (RRBCs) and antibody-containing serum/plasma onto a gel card containing separation media, incubating the card for 5−15 min and using a centrifuge to separate agglutinated cells from free cells (Figure 1A), resulting in strong red lines on top of the gel column in the case of a "positive" test. A wide range of RRBCs expressing different surface antigens are available for assay development, along with corresponding antibodies of varying affinity and avidity. During the early years of the human immunodeficiency virus (HIV) epidemic, Kemp et al. developed a variant of the blood typing assays to detect HIV-induced antibodies present in the blood of previously infected patients.[15] Antiglycophorin antibodies or Fabs[16] were bioconjugated to viral peptide gp41 so that, in the presence of a human blood sample, the antibodies would bind any red blood cells (RBCs), while the peptide would bind to anti-HIV-IgG, producing agglutination reactions only in the presence of blood plasma collected from HIV-positive people. The degree of agglutination was then read on a microscope slide by a trained reader. However, to automate the process and broadly deploy this approach, an alternative to microscopic examination of agglutination reactions is required.

In this study, we developed a serology test to detect SARS-CoV-2 antibodies from human plasma using gel card agglutination tests. The CAT technology was selected for rapid and high throughput testing and comprehensive serology mapping, for two reasons. First, CAT is currently available in the blood/analytical laboratory of all major hospitals throughout the world as an automated and high throughput platform (>100 tests/h), with equipment and trained personnel already in place. Second, many companies are currently manufacturing the gel cards widely used for blood typing analysis. Production of SARS-CoV-2 gel card diagnostics only requires the substitution of the current RRBCs with bioconjugated cells, using the current processing and technology. We have found that by producing bioconjugates of anti-D-IgG and peptides from SARS-CoV-2 spike protein, and immobilizing these to RRBCs, we observe selective

https://dx.doi.org/10.1021/acssensors.0c01050
ACS Sens. XXXX, XXX, XXX−XXX

agglutination assays in gel cards in the presence of plasma collected from patients recently infected with SARS-CoV-2 in comparison to healthy plasma and negative controls.

MATERIALS AND METHODS

Materials. Chemicals were purchased from Sigma-Aldrich unless otherwise identified. Seeblue plus2 protein standard (Thermo Fisher Scientific), GelCode blue stain reagent (Thermo Fisher Scientific), goat anti-human IgG (H + L), cross-adsorbed secondary antibody, HRP-labeled (Thermo Fisher Scientific), gel apparatus (Life Technology), PBS (Gibco, Invitrogen), syringe filters (0.22−0.45 μm, Pall, Inc.), HiTrap Protein A column (GE Healthcare), anti-D-IgG FFMU ("for further manufacturing use", Immulab), NHS-(PEG)2-maleimide (Quanta Biodesign), zebapsin columns (7K MWCO, Thermo Fisher Scientific), and Celpresol (Immulab).

Anti-D-IgG Purification and Bioconjugation Reaction. Anti-D-IgG was purified from FFMU product using Protein A affinity chromatography and buffer exchange. The FFMU (100 mL) was filtered through a 0.22 μm filter before being loaded onto the purification column. A HiTrap Protein A column (GE Healthcare) was connected to AKTA Chromatography System (AKTA Start, GE Healthcare), equilibrated with 1X PBS buffer (pH 7.4). The filtered supernatant was loaded onto the column followed by washing with 1X PBS (3 column volume). Proteins were eluted using glycine elution buffer (1X PBS, 0.1 M glycine, pH 2.8), neutralized by adding 150 μL of 1 M Tris pH 9 per 1 mL eluate, and then exchanged to 1× PBS buffer (pH 7.4) using a HiPrep 26/10 desalting column. The resulting purified anti-D-IgG was then concentrated and stored at 4 °C for several weeks, over which time we observed no precipitation or reduction in absorbance at 280 nm as measured on a Nanodrop spectrometer.

Peptide Synthesis. Peptides were synthesized via a microwave-assisted solid-phase synthesis using Rink amide resin (0.05 mmol scale, 100−200 mesh, 1% DVB, ChemPep, Inc.) as the resin. Syntheses were performed in an automated microwave synthesizer (Liberty Blue, CEM Corporation, North Carolina). Resin was swelled at room temperature for 5 min with *N*,*N*-dimethylformamide (DMF) before deprotection with 20% 4-methylpiperidine in DMF (v/v) for 30 s at 75 °C and 90 s at 90 °C. Subsequently, Fmoc amino acids (0.25 mmol, ChemPep, Inc.) were coupled with a 1:1:1:2 ratio of amino acid/1-hydroxybenzotriazole hydrate (HOBT, AK Scientific, Inc.)/HCTU (AK Scientific, Inc.)/*N*,*N*-diisopropylethylamine (DIPEA) in 4 mL of DMF at 70 °C for 5 min prior to deprotection with 20% 4-methylpiperidine in DMF (v/v) for 5 min at 75 °C. Fluorescein was included in the N-terminal region by coupling of 5,6-carboxyfluoroscein (0.25 mmol) to the final amino acid in the sequence, after Fmoc deprotection, with a 1:1:1:2 ratio of amino acid/HOBT/HCTU/DIPEA in 4 mL of DMF at 70 °C. The fluorescein coupling step was performed twice to ensure complete labeling of the synthesized sequences.

After solid-phase synthesis, the resultant dried Rink amide resin was transferred to a 25 mL solid-phase peptide synthesis vessel (CG-1866, Chemglass) and treated with 10 mL of trifluoroacetic acid (TFA)/phenol/water/triisopropylsilane (88/5/5/2) cleavage cocktail for 2 h while bubbling with nitrogen at room temperature. The TFA cleavage solution was collected by filtering through the fritted glass into a 25 mL round-bottom flask. The remaining resin was further rinsed twice with 5 mL of fresh TFA cleavage cocktail to collect any residual peptoid. The cleavage solution was combined and precipitated into cold diethyl ether. Upon centrifugation, the precipitate was collected and reconstituted in HPLC grade water/acetonitrile (MeCN) with 0.1% TFA. Peptides were purified by preparative HPLC using a linear gradient of MeCN and water: (1) 10% MeCN, 0.1−2.1 min; (2) 10−95% MeCN, 2.1−23.1.1 min; (3) 95% MeCN, 23.1−26.1 min. Purified peptides were lyophilized to yield off-white powder and characterized by electrospray ionization-mass spectrometry (ESI-MS).

Bioconjugate Reaction. Bioconjugation reactions were performed with ∼3 mg/mL anti-D-IgG concentrations at 100 μL scale. 50-fold molar excess of NHS−$(PEG)_2$−maleimide was added to the antibody and incubated for 2 h at 4 °C. This mixture was then desalted using Zebaspin columns to remove the free PEG, before reaction with peptide. The thiolated peptide was added to the antibody solution in 15−20-fold molar excess, incubated at room temperature for 1 h, before another desalting step to remove free peptide. The resulting bioconjugates were loaded into NuPage 4−12% Bis-Tris gels for SDS-PAGE analysis in accordance with the manufacturer's instructions. The gels were analyzed in a UVP Biospectrum gel imager using Cy2 excitation/emission filters to confirm antibody labeling with the fluorescent peptide, prior to Coomassie staining (GelCode) and imaging under white light. Bioconjugates were stored in 1× PBS stocks at 4 °C and were stable for at least several weeks. Concentrations of bioconjugates were monitored using a Nanodrop spectrometer.

Flow Cytometry. Flow assays were performed to confirm bioconjugate binding to RRBCs and to determine the concentration of biconjugate required to saturate the cells. Data were collected on a Beckman Coulter Cytoflex. A single gate identifying the RRBCs on a forward/side scatter plot was applied to the fluorescence histogram displaying FAM-positive cells. Data were exported to FlowJo LLC for off-line analysis and plotted for display in GraphPad Prism.

Column Agglutination Tests. Stocks of bioconjugate-labeled RRBCs (R2R2 cells) were prepared fresh daily. RRBCs (0.8%) in healthy human plasma solution were prepared, and bioconjugate was added directly to achieve the desired ratio of bioconjugate/D-antigen on the cells. Following 20 min incubation at room temperature, the cells were pelleted and washed four times in Celpresol solution. Neutral cards produced by Haemokinesis were employed as required for CAT assays unless otherwise noted. Bioconjugate-coated RRBCs (0.8%, 50 μL; unless otherwise stated, a 2:1 bioconjugate/D-antigen ratio was used) were added to the gel cards along with 25 μL of plasma. The cards were incubated at 25 °C for 10 min (with an extra 5 min incubation at 4 °C for Figure 4), then centrifuged for 11 min (Haemokinesis gel card centrifuge), and the results were recorded digitally using the Haemokinesis gel card reader. Deidentified human plasma or serum samples were provided by Monash Pathology and the Australian Red Cross Lifeblood, obtained with written informed consent in accordance with the recommendations of Blood Service Human Research Ethics Committee (BSHREC) and the Monash University Human Research Ethics Committee (MUHREC).

Indirect IgG ELISA. A mixture of recombinant spike S1, spike S1 + S2, spike-RBD (Receptor Binding Domain), and nucleocapsid proteins from SARS-CoV-2 (mass ratio 1:1:1:0.5; Jomar Life Research) was coated in 96-well plates (Nunc flat bottom, Maxisorp; 0.22 μg/mL total protein concentration) and incubated overnight at 4 °C. Plates were blocked with 200 μL of a blocking buffer (5% skim milk diluent in 1X PBS) for 2 h at room temperature. Plasma samples were then diluted into a dilution buffer (5% skim milk diluent in 1× PBS/0.05% Tween-20, herein referred to as "PBST") and titrated down the plate at 50 μL/well. After 1 h incubation at 37 °C, the wells were washed six times with PBST. Anti-IgG-HRP antibody was diluted into PBST (1:15 000), and 50 μL was added to each well. After a 60 min incubation at 37 °C, the wells were washed six times with PBST. 3,3′,5,5′-Tetramethylbenzidine (TMB, 50 μL, Thermo Fisher Scientific) was then added to each well, followed by 1 M hydrochloric acid as a stopping solution. The colorimetric reaction was analyzed by recording the absorbance at 450 nm in a Tecan Infinite M Nano plate reader, and the results were plotted for display in GraphPad Prism. The limit of quantification (LOQ) was defined here as three standard deviations above the mean signal from wells tested without plasma (0.065 absorbance units).

RESULTS AND DISCUSSION

We designed a SARS-CoV-2-specific serology assay using an agglutination approach, based on the widespread availability of the simple CAT technology commonly employed for blood typing (Figure 1). In a standard blood typing assay, patients' RBCs and plasma are separately reacted with reagent

https://dx.doi.org/10.1021/acssensors.0c01050
ACS Sens. XXXX, XXX, XXX−XXX

antibodies or RBCs, respectively, in gel cards to identify a specific blood type. When RBCs agglutinate, they cannot pass through the gel card, and hence a visible red line is observed following card centrifugation. In Figure 1A, agglutination of (i) patient RBCs with reagent anti-A-IgM and anti-D-IgM and (ii) patient antibodies with B+ reagent cells confirms the A+ blood type. In contrast, we introduced an antibody−peptide bioconjugate (Figure 1B) that would aggregate RRBCs only in the presence of antibodies against SARS-CoV-2 (Figure 1C). We selected anti-D-IgG as the antibody scaffold, based on its strong affinity for the Rh D-antigen on R2R2 cells. Peptides from the SARS-CoV-2 spike protein were selected based on emerging computational and experimental epitope mapping studies[17] and synthesized via automated solid-phase peptide synthesis (SPSS) with C-terminal cysteine tags and N-terminal FAM labels (Figure S1). The bioconjugation process consisted of reacting NHS-PEG(2)-maleimide with the lysine side chains of nonreduced anti-D-IgG, then coupling the cysteine-terminated peptide to the maleimide-tagged antibodies via thioether bonds.

Antibody−peptide bioconjugates were designed to bind SARS-CoV-2-specific antibodies raised in response to viral infection. Peptides were selected based on early predictions from database mining projects, where P1, P2, and P5 are all elements of the SARS-CoV-2 spike protein (Figure S1). Following the crude purification of anti-D-IgG (Figure S2) and the simple bioconjugation procedure outlined in Figure 1B, the bioconjugates were analyzed by gel electrophoresis to confirm peptide labeling. Fluorescence analysis revealed clear bands ∼150 kDa only for those samples labeled with FAM (fluorescein amidite), with no evidence of fluorescence emission for the anti-D-IgG control (Figure 2A). After staining the same gel with Coomassie Blue, all four bioconjugates were clearly visible, confirming successful peptide labeling (Figure 2B). The labeling efficiency was estimated at 5−10% based on Nanodrop analysis, from ∼10- to 20-fold molar excess of peptide, above which we observed evidence of protein precipitation, in agreement with previous studies.[15] While the labeling efficiency was lower than expected, the gels showed some evidence of impurities in the purified anti-D-IgG sample, and the FAM incorporation into peptides may not be 100% as the dye incorporation is the final step in the peptide synthesis process. As expected, the bioconjugates bound RRBCs efficiently, showing strong and titratable FAM intensity in flow cytometry (Figure 2C). Saturation occurred at a bioconjugate/cell ratio of 1-2:1, and it was later found that maintaining this ratio in gel card assays was critical to forming clear agglutination signal.

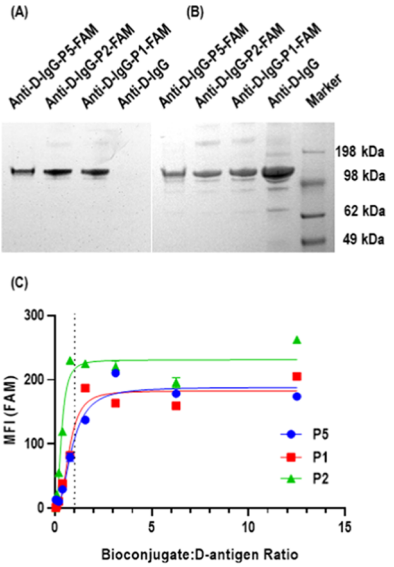

Figure 2. Anti-D-IgG−peptide bioconjugate characterization. (A) Fluorescence scan of protein gel under Cy2 filter. (B) Bright-field image of the same gel following Coomassie staining. (C) Graph showing the bioconjugate binding to Rh D-antigen positive RRBCs using flow cytometry, and the effect of bioconjugate titration. The dotted line indicates equimolar bioconjugate and D-antigen in the incubation reaction.

We next investigated the agglutination potential of bioconjugate-coated RRBCs. To ensure that the bioconjugate did not inhibit the potential for RRBCs to agglutinate, we first incubated bioconjugate-coated RRBCs with anti-IgG antibodies prior to centrifugation (Figure 3A).[18] While RRBCs alone

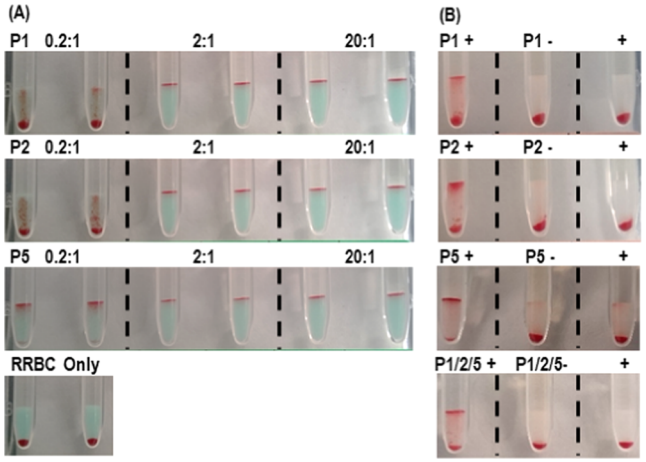

Figure 3. Optimization of gel card assays for SARS-CoV-2 serology. (A) Testing the ability of bioconjugates to cross-link RRBCs independent of attached peptide, using anti-IgG in PBS. "P*n*" indicates the peptide used in the reactions (n = 1, 2, or 5), and the ratios indicate the bioconjugate to D-antigen (on cells). (B) Selective agglutination of SARS-CoV-2 antibodies present in a clinical sample in comparison to negative controls, using bioconjugate-saturated RRBCs. Reactions involving SARS-CoV-2-positive samples indicated by "+" and SARS-CoV-2-negative samples indicated by "−". Samples labelled only as "+" indicate SARS-CoV-2 positive samples incubated with RRBCs in the absence of bioconjugates. Reactions labeled "P1/2/5" indicate that bioconjugate-coated RRBCs were mixed to provide the same total peptide concentration as used for other reactions.

spun through the gel card as a negative control, if the RRBCs were saturated with bioconjugate (i.e., bioconjugate/D-antigen ratio > 1:1), we observed strong agglutination with no evidence of free cells traveling through the gel card. If the RRBCs were not saturated (e.g., 0.2:1 ratio), we observed only partial agglutination in, or on top of, the gel columns, presumably because there was not sufficient bioconjugate present to cross-link cells with the anti-IgG ("Coombs' reagent"). This suggested that operating the assays under conditions of bioconjugate saturation is required for successful agglutination and retention of aggregated cells above the gel column.

We next progressed to optimize gel card agglutination assays to distinguish between SARS-CoV-2-positive and SARS-CoV-2-negative patient samples. Preliminary optimization experi-

https://dx.doi.org/10.1021/acssensors.0c01050
ACS Sens. XXXX, XXX, XXX−XXX

ments suggested that common protocols used in blood typing assays were also appropriate for SARS-CoV-2 serology assays, i.e., 5−10 min incubation of gel cards at 25 °C, followed by 11 min centrifugation. Consistent with our findings related to Figure 3A, a significant factor affecting the degree of agglutination was the bioconjugate:cell ratio. If this ratio was not high enough to ensure cell saturation, a higher proportion of RRBCs was observed to pellet upon centrifugation. When using saturated bioconjugate-cell reagents, we were able to detect positive agglutination results with each of the three bioconjugates tested. Importantly, negative control reactions involving either SARS-CoV-2-negative samples or RRBCs and SARS-CoV-2-positive samples without bioconjugates all revealed no agglutination behavior. Only rarely did we observe "complete" agglutination (with no cells pelleted following centrifugation), which was expected because not all cell-bound antibodies were tagged with peptide. Reactions involving mixed bioconjugates (mixtures prepared after cell incubation) were also tested, showing similar results to those for single-bioconjugate reactions, which is important, as we expect that multiple immunodominant peptides will be required to minimize false positives in large cohorts. Importantly, during the optimization phase of assay development, we occasionally observed false-positive results, i.e., a red line appearing above the gel column after incubation of bioconjugate-coated RRBCs and SARS-CoV-2-negative plasma. However, upon microscopy, it was revealed that these cells were not agglutinated (Figure S3); this was mainly related to the presence of glycerol carried over from the bioconjugate stock solution. While 1:1 glycerol/PBS mixtures are commonly used for long-term −20 °C storage of bioconjugates, the glycerol carryover into RRBCs for agglutination reaction should be minimized or removed.

Following optimization of the gel card assays to distinguish between SARS-CoV-2-positive samples and negative controls, we tested 10 clinical samples in both gel cards and indirect IgG ELISA (Figure 4). The ELISA was designed to capture and detect IgG antibodies from plasma which bound to SARS-CoV-2 proteins coated onto the plates. This assay cannot detect IgM antibodies, which are also likely to be present in many samples;[10] however, we expect that IgM levels are likely to recede over time in at least some individuals, whereas IgG levels are likely to remain high over time and hence are appropriate to confirm immune response to infection. We observed strong IgG signals for all five PCR-confirmed SARS-CoV-2-positive samples, while all negative samples revealed signals at or below the LOQ for the assay (Figure 4A). Given that samples used for serology testing contain a unique and complex polyclonal mixture of IgG and IgM antibodies, it is not meaningful to calibrate or quantify relative to a standard; hence, the data are regularly reported based on dilutions or titers.[10−12] Notably, one of the positive samples was collected only 8 days post PCR, suggesting that the assay may be capable of detecting IgG levels well before they are expected to peak (~19 days[10]). Importantly, the SARS-CoV-2-negative samples tested were collected prior to the pandemic (Table S1), as it is possible that samples collected from apparently healthy people during the pandemic could indeed be from asymptomatic carriers. We then tested the same 10 samples in gel card agglutination tests using a mixture of all three bioconjugates and included negative controls for which RRBCs were not coated with bioconjugates. Here, we added an additional 5 min incubation step at 4 °C prior to centrifugation as this is one way of enhancing agglutination reactions to achieve strongly

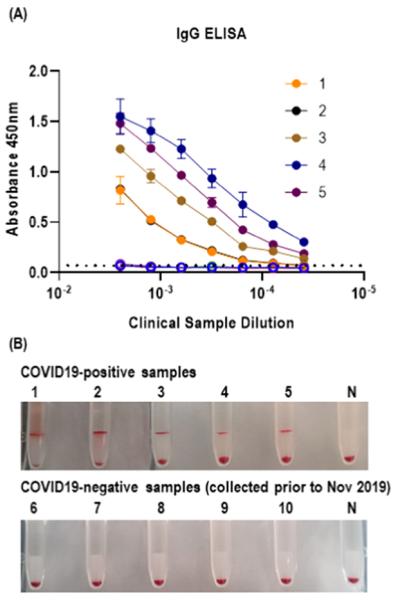

Figure 4. Clinical sample analysis comparing indirect IgG ELISA against agglutination approach using RRBCs coated with P1, P2, and P5 bioconjugates prior to mixing. (A) Indirect IgG ELISA results comparing five PCR-confirmed SARS-CoV-2-positive samples (filled circles) against five samples collected from healthy individuals prior to SARS-CoV-2 pandemic (empty circles). The dotted line indicates the limit of quantification (LOQ) for the assay, determined to be three standard deviations above wells containing PBST instead of clinical sample. (B) Digital images of gel card assays comparing five PCR-confirmed SARS-CoV-2-positive samples against five samples collected from healthy individuals prior to the SARS-CoV-2 pandemic. Negative control ("N") tests were performed using RRBCs and clinical sample (sample 5 for positives; sample 10 for negatives) without bioconjugates.

visible bands across a range of samples. The same effect could likely be achieved using agglutination-enhancing solutions, including low-ionic-strength saline (LISS). All five PCR-confirmed SARS-CoV-2-positive samples yielded positive agglutination results, while the negative samples showed no agglutination above the gel (Figure 4B). The lack of positive results in ELISA or agglutination tests for these negative samples is particularly encouraging, because in a recent study, four out of five SARS-CoV-2-negative blood samples showed high levels of antibodies against seasonal coronaviruses but no cross-reactive antibodies that bind SARS-CoV-2.[19] This is consistent with earlier estimates that nearly 100% of adolescents have antibodies against seasonal coronaviruses.[20] This analysis shows that the gel card agglutination tests can provide serological results for SARS-CoV-2 infection within 30 min, using an approach consistent with blood typing assays used routinely in hospital labs around the world.

In this study, we have taken widely used blood typing tests and converted them into SARS-CoV-2 serology tests. Given the rapid turnaround time, high throughput, and level of clinical acceptance, we suggest that with further testing in large sample cohorts to accurately characterize false-positive/-negative rates, CAT assays could provide an alternative to ELISAs. At the time of writing this manuscript, there is still much to learn about SARS-CoV-2 virology, the nature and spectrum of immune responses, and the utility of serology assays as the pandemic runs its course internationally. Key limitations at present include the lack of knowledge on which

https://dx.doi.org/10.1021/acssensors.0c01050
ACS Sens. XXXX, XXX, XXX−XXX

SARS-CoV-2 peptides are immunodominant, whether or not predicted B-cell epitopes will efficiently bind antibodies (IgG, IgM, etc.) in patient blood, and what is the level of cross-reactivity between antibodies raised against previous coronavirus infections in large sample cohorts. It is also unclear if distinguishing between IgM and IgG would be clinically relevant, given the lack of consistent class switching trends reported to date; however, it would likely be relevant in terms of understanding the immune response in more detail. One recent study used a peptide microarray to determine IgG/IgM binding epitopes from the blood of 40 infected individuals and identified that 80% of the samples contained both IgG and IgM antibodies against just four epitope sequences (which includes our current P2 peptide).[21] This confirms that pursuing an approach involving multiple bioconjugates is likely required to minimize false-negative results in large sample cohorts. An alternative approach would be to create bioconjugates using whole proteins instead of peptide epitopes; the advantage would be that protein sequences are often much faster to determine in comparison to identifying a minimal list of immunodominant peptides, which is important in terms of pandemic response. However, bioconjugation reactions involving whole (and potentially novel) proteins are likely to be less efficient due to size/charge comparisons, requiring individual tailoring of reaction conditions, whereas many peptide bioconjugates can be prepared simultaneously.

CONCLUSIONS

In this study, we have transformed blood typing tests into SARS-CoV-2 serology tests using robust gel card agglutination reactions in combination with easily prepared antibody−peptide bioconjugates. We found concordance between results for gel card assays and an indirect IgG ELISA across 10 clinical samples, five of which were PCR-confirmed SARS-CoV-2-positive samples. During assay development, we found that it was critical to ensure that RRBCs were saturated with bioconjugates; otherwise, agglutination did not occur or was extremely inefficient. We also found that very small amounts of glycerol in the RRBC cell stocks caused false-positive results; hence, care must be taken when choosing buffer and storage solutions to investigate the effects of all additives. This assay was designed and operated based on the infrastructure routinely available in blood typing laboratories worldwide, and this approach is now ready to be evaluated for clinical application with a large sample cohort, leading to the next phase of industry partnership for scale-up and distribution.

ASSOCIATED CONTENT

Supporting Information

The Supporting Information is available free of charge at https://pubs.acs.org/doi/10.1021/acssensors.0c01050.

LC/MS analysis of synthesized peptides (Figure S1); SDS-PAGE gel for anti-D-IgG purification (Figure S2); optical microscopy images distinguishing true/false-positive gel card results (Figure S3); and list of clinical samples used in the study (Table S1) (PDF)

AUTHOR INFORMATION

Corresponding Authors

Gil Garnier − *Department of Chemical Engineering, ARC Centre of Excellence in Convergent BioNano Science and Technology and Bioresource Processing Research Institute of Australia (BioPRIA), Monash University, Clayton, Victoria 3800, Australia;* orcid.org/0000-0003-3512-0056; Email: gil.garnier@monash.edu

Simon R. Corrie − *Department of Chemical Engineering, ARC Centre of Excellence in Convergent BioNano Science and Technology, Bioresource Processing Research Institute of Australia (BioPRIA), Centre to Impact AMR, and Monash Institute of Pharmaceutical Sciences, Monash University, Clayton, Victoria 3800, Australia;* orcid.org/0000-0001-8029-1896; Email: simon.corrie@monash.edu

Authors

Diana Alves − *Department of Chemical Engineering, ARC Centre of Excellence in Convergent BioNano Science and Technology and Bioresource Processing Research Institute of Australia (BioPRIA), Monash University, Clayton, Victoria 3800, Australia*

Rodrigo Curvello − *Department of Chemical Engineering, ARC Centre of Excellence in Convergent BioNano Science and Technology and Bioresource Processing Research Institute of Australia (BioPRIA), Monash University, Clayton, Victoria 3800, Australia*

Edward Henderson − *Department of Chemical Engineering, ARC Centre of Excellence in Convergent BioNano Science and Technology, Bioresource Processing Research Institute of Australia (BioPRIA), and Centre to Impact AMR, Monash University, Clayton, Victoria 3800, Australia*

Vidhishri Kesarwani − *Department of Chemical Engineering, ARC Centre of Excellence in Convergent BioNano Science and Technology, Bioresource Processing Research Institute of Australia (BioPRIA), and Centre to Impact AMR, Monash University, Clayton, Victoria 3800, Australia*

Julia A. Walker − *Department of Chemical Engineering, ARC Centre of Excellence in Convergent BioNano Science and Technology, Bioresource Processing Research Institute of Australia (BioPRIA), Centre to Impact AMR, and Monash Institute of Pharmaceutical Sciences, Monash University, Clayton, Victoria 3800, Australia*

Samuel C. Leguizamon − *Department of Chemical Engineering, ARC Centre of Excellence in Convergent BioNano Science and Technology, Bioresource Processing Research Institute of Australia (BioPRIA), and Department of Materials Science and Engineering, Monash University, Clayton, Victoria 3800, Australia; Department of Chemical Engineering, University of Michigan, Ann Arbor, Michigan 48109, United States*

Heather McLiesh − *Department of Chemical Engineering, ARC Centre of Excellence in Convergent BioNano Science and Technology and Bioresource Processing Research Institute of Australia (BioPRIA), Monash University, Clayton, Victoria 3800, Australia*

Vikram Singh Raghuwanshi − *Department of Chemical Engineering, ARC Centre of Excellence in Convergent BioNano Science and Technology and Bioresource Processing Research Institute of Australia (BioPRIA), Monash University, Clayton, Victoria 3800, Australia*

Hajar Samadian − *Department of Chemical Engineering, ARC Centre of Excellence in Convergent BioNano Science and Technology and Bioresource Processing Research Institute of Australia (BioPRIA), Monash University, Clayton, Victoria 3800, Australia*

Erica M. Wood − *Department of Clinical Haematology, Monash Health, Clayton, Victoria 3168, Australia; Department of*

https://dx.doi.org/10.1021/acssensors.0c01050
ACS Sens. XXXX, XXX, XXX−XXX

Epidemiology and Preventive Medicine, Monash University, Melbourne, Victoria 3004, Australia

Zoe K. McQuilten − *Department of Clinical Haematology, Monash Health, Clayton, Victoria 3168, Australia; Department of Epidemiology and Preventive Medicine, Monash University, Melbourne, Victoria 3004, Australia*

Maryza Graham − *Department of Microbiology and Monash Infectious Diseases, Monash Health, Clayton, Victoria 3168, Australia; Department of Clinical Sciences, Monash University, Clayton, Victoria 3168, Australia*

Megan Wieringa − *Department of Microbiology, Monash Health, Clayton, Victoria 3168, Australia; Department of Clinical Sciences, Monash University, Clayton, Victoria 3168, Australia*

Tony M. Korman − *Department of Microbiology and Monash Infectious Diseases, Monash Health, Clayton, Victoria 3168, Australia; Center for Inflammatory Diseases, Department of Medicine, Monash University, Clayton, Victoria 3800, Australia*

Timothy F. Scott − *Department of Chemical Engineering, ARC Centre of Excellence in Convergent BioNano Science and Technology, Bioresource Processing Research Institute of Australia (BioPRIA), and Department of Materials Science and Engineering, Monash University, Clayton, Victoria 3800, Australia;* orcid.org/0000-0002-5893-3140

Mark M. Banaszak Holl − *Department of Chemical Engineering, ARC Centre of Excellence in Convergent BioNano Science and Technology and Bioresource Processing Research Institute of Australia (BioPRIA), Monash University, Clayton, Victoria 3800, Australia;* orcid.org/0000-0001-7759-7456

Complete contact information is available at: https://pubs.acs.org/10.1021/acssensors.0c01050

Author Contributions

D.A., R.C., E.H., V.K., J.A.W., S.C.L., H.M, V.S.R., and H.S. contributed equally. The manuscript was written through contributions of all authors. All authors have given approval to the final version of the manuscript.

Notes

The authors declare no competing financial interest.

■ ACKNOWLEDGMENTS

The authors acknowledge funding support from the Chemical Engineering Department and the Centre to Impact Anti-Microbial Resistance at Monash University to undertake this project. They also acknowledge the Australian Red Cross Lifeblood for providing clinical samples.

■ REFERENCES

(1) Coronavirus Update (Live), Worldometer. https://www.worldometers.info/coronavirus/.

(2) Australian Government Department of Health. https://www.health.gov.au/news/health-alerts/novel-coronavirus-2019-ncov-health-alert#current-status.

(3) Carter, L. J.; Garner, L. V.; Smoot, J. W.; Li, Y.; Zhou, Q.; Saveson, C. J.; Sasso, J. M.; Gregg, A. C.; Soares, D. J.; Beskid, T. R.; Jervey, S. R.; Liu, C. Assay Techniques and Test Development for COVID-19 Diagnosis. *ACS Cent. Sci.* **2020**, *6*, 591−605.

(4) Udugama, B.; Kadhiresan, P.; Kozlowski, H. N.; Malekjahani, A.; Osborne, M.; Li, V. Y. C.; Chen, H.; Mubareka, S.; Gubbay, J. B.; Chan, W. C. W. Diagnosing COVID-19: The Disease and Tools for Detection. *ACS Nano* **2020**, *14*, 3822−3835.

(5) Seo, G.; Lee, G.; Kim, M. J.; Baek, S.-H.; Choi, M.; Ku, K. B.; Lee, C.-S.; Jun, S.; Park, D.; Kim, H. G.; Kim, S.-J.; Lee, J.-O.; Kim, B. T.; Park, E. C.; Kim, S. I. Rapid Detection of COVID-19 Causative Virus (SARS-CoV-2) in Human Nasopharyngeal Swab Specimens Using Field-Effect Transistor-Based Biosensor. *ACS Sensors* **2020**, *14*, 5135−5142.

(6) Qiu, G.; Gai, Z.; Tao, Y.; Schmitt, J.; Kullak-Ublick, G. A.; Wang, J. Dual-Functional Plasmonic Photothermal Biosensors for Highly Accurate Severe Acute Respiratory Syndrome Coronavirus 2 Detection. *ACS Sensors* **2020**, *14*, 5268−5277.

(7) Lipsitch, M.; Kahn, R.; Mina, M. J. Antibody testing will enhance the power and accuracy of COVID-19-prevention trials. *Nat. Med.* **2020**, *26*, No. 818819.

(8) Lee, C. Y.-P.; Lin, R. T. P.; Renia, L.; Ng, L. F. P. Serological Approaches for COVID-19: Epidemiologic Perspective on Surveillance and Control | Immunology. *Front. Immunol.* **2020**, *11*, No. 879.

(9) Winter, A. K.; Hegde, S. T. The important role of serology for COVID-19 control - The Lancet Infectious Diseases. *Lancet Infect. Dis.* **2020**, *20*, 758−759.

(10) Long, Q.-X.; Liu, B.-Z.; Deng, H.-J.; Wu, G.-C.; Deng, K.; Chen, Y.-K.; Liao, P.; Qiu, J.-F.; Lin, Y.; Cai, X.-F.; Wang, D.-Q.; Hu, Y.; Ren, J.-H.; Tang, N.; Xu, Y.-Y.; Yu, L.-H.; Mo, Z.; Gong, F.; Zhang, X.-L.; Tian, W.-G.; Hu, L.; Zhang, X.-X.; Xiang, J.-L.; Du, H.-X.; Liu, H.-W.; Lang, C.-H.; Luo, X.-H.; Wu, S.-B.; Cui, X.-P.; Zhou, Z.; Zhu, M.-M.; Wang, J.; Xue, C.-J.; Li, X.-F.; Wang, L.; Li, Z.-J.; Wang, K.; Niu, C.-C.; Yang, Q.-J.; Tang, X.-J.; Zhang, Y.; Liu, X.-M.; Li, J.-J.; Zhang, D.-C.; Zhang, F.; Liu, P.; Yuan, J.; Li, Q.; Hu, J.-L.; Chen, J.; Huang, A.-L. Antibody responses to SARS-CoV-2 in patients with COVID-19. *Nat. Med.* **2020**, *26*, 845−848.

(11) Assis, R. R. d.; Jain, A.; Nakajima, R.; Jasinskas, A.; Felgner, J.; Obiero, J. M.; Adenaiye, O.; Tai, S.; Hong, F.; Norris, P. J.; Stone, M.; Simmons, G.; Bagri, A.; Schreiber, M.; Buser, A.; Holbro, A.; Battegay, M.; Hosimer, P.; Noesen, C.; Milton, D. K.; Group, P. S.; Davies, D. H.; Contestable, P.; Corash, L. M.; Busch, M. P.; Felgner, P. L.; Khan, S. Analysis of SARS-CoV-2 Antibodies in COVID-19 Convalescent Blood using a Coronavirus Antigen Microarray. *bioRxiv* **2020**, DOI: 10.1101/2020.04.15.043364.

(12) To, K. K.-W.; Tsang, O. T.-Y.; Leung, W.-S.; Tam, A. R.; Wu, T.-C.; Lung, D. C.; Yip, C. C.-Y.; Cai, J.-P.; Chan, J. M.-C.; Chik, T. S.-H.; Lau, D. P.-L.; Choi, C. Y.-C.; Chen, L.-L.; Chan, W.-M.; Chan, K.-H.; Ip, J. D.; Ng, A. C.-K.; Poon, R. W.-S.; Luo, C.-T.; Cheng, V. C.-C.; Chan, J. F.-W.; Hung, I. F.-N.; Chen, Z.; Chen, H.; Yuen, K.-Y. Temporal profiles of viral load in posterior oropharyngeal saliva samples and serum antibody responses during infection by SARS-CoV-2: an observational cohort study - The Lancet Infectious Diseases. *Lancet Infect. Dis.* **2020**, *20*, 565−574.

(13) Bryan, A.; Pepper, G.; Wener, M. H.; Fink, S. L.; Morishima, C.; Chaudhary, A.; Jerome, K. R.; Mathias, P. C.; Greninger, A. L. Performance Characteristics of the Abbott Architect SARS-CoV-2 IgG Assay and Seroprevalence in Boise, Idaho. *J. Clin. Microbiol.* **2020**, No. 00941-20.

(14) Mabey, D.; Peeling, R. W.; Ustianowski, A.; Perkins, M. D. Diagnostics for the developing world. *Nat. Rev. Microbiol.* **2004**, *2*, 231−240.

(15) Kemp, B.; Rylatt, D.; Bundesen, P.; Doherty, R.; McPhee, D.; Stapleton, D.; Cottis, L.; Wilson, K.; John, M.; Khan, J.; et al. Autologous red cell agglutination assay for HIV-1 antibodies: simplified test with whole blood. *Science* **1988**, *241*, 1352−1354.

(16) Wilson, K. M.; Gerometta, M.; Rylatt, D. B.; Bundesen, P. G.; McPhee, D. A.; Hillyard, C. J.; Kemp, B. E. Rapid whole-blood assay for HIV-1 seropositivity using an Fab-peptide conjugate. *J. Immunol. Methods* **1991**, *138*, 111−119.

(17) Grifoni, A.; Sidney, J.; Zhang, Y.; Scheuermann, R. H.; Peters, B.; Sette, A. A Sequence Homology and Bioinformatic Approach Can Predict Candidate Targets for Immune Responses to SARS-CoV-2. *Cell Host Microbe* **2020**, *27*, 671−680.

(18) Yeow, N.; McLiesh, H.; Guan, L.; Shen, W.; Garnier, G. Paper-based Assay for Red Blood Cell Antigen Typing by the Indirect Antiglobulin Test. *Anal. Bioanal. Chem.* **2016**, *408*, 5231−5238.

(19) Khan, S.; Nakajima, R.; Jain, A.; de Assis, R. R.; Jasinskas, A.; Obiero, J. M.; Adenaiye, O.; Tai, S.; Hong, F.; Milton, D. K.; Davies,

H.; Felgner, P. L. Analysis of Serologic Cross-Reactivity Between Common Human Coronaviruses and SARS-CoV-2 Using Coronavirus Antigen Microarray. *bioRxiv* **2020**, DOI: 10.1101/2020.03.24.006544.

(20) Zhou, W.; Wang, W.; Wang, H.; Lu, R.; Tan, W. First infection by all four non-severe acute respiratory syndrome human coronaviruses takes place during childhood. *BMC Infect. Dis.* **2013**, *13*, No. 433.

(21) Wang, H.; Hou, X.; Wu, X.; Liang, T.; Zhang, X.; Wang, D.; Teng, F.; Dai, J.; Duan, H.; Guo, S.; Li, Y.; Yu, X. SARS-CoV-2 proteome microarray for mapping COVID-19 antibody interactions at amino acid resolution. *bioRxiv* **2020**, DOI: 10.1101/2020.03.26.994756.

https://dx.doi.org/10.1021/acssensors.0c01050
ACS Sens. XXXX, XXX, XXX−XXX